SUNDIAL : a world-wide-study of interactive ionospheric processes and their roles in the transfer of energy and mass in the Sun-Earth system

E. P. SZUSZCZEWICZ ([1]), B. FEJER ([2]), E. ROELOF ([3]), R. SCHUNK ([4]), R. WOLF ([5]), R. LEITINGER ([6]), M. ABDU ([7]), B. M. REDDY ([8]), J. JOSELYN ([9]), P. WILKINSON ([10]) and R. WOODMAN ([11])

([1]) *Science Applications International Corporation, McLean, Virginia* 22102, *U.S.A.*
([2]) *Cornell University, U.S.A.* ([3]) *Johns Hopkins University U.S.A.*
([4]) *Utah State University, U.S.A.* ([5]) *Rice University, U.S.A.*
([6]) *Universitaet Graz, Austria.* ([7]) *INPE, Brazil.* ([8]) *NPL, India*
([9]) *NOAA, U.S.A.* ([10]) *IPS, Australia.* ([11]) *IGP, Peru*

Received February 27, 1987 ; revised June 24, 1987 ; accepted August 12, 1987.

ABSTRACT. During the period 5-13 October 1984 a coordinated solar-terrestrial data base was acquired to develop a comprehensive understanding and an associated predictive capability for the cause-effect relationships which control the global-scale ionosphere. The effort, the first in a series of continuing investigations in a program called SUNDIAL, combined modelling of the ionospheric, magnetospheric, and thermospheric domains with a measurements activity that included a network of ionospheric monitoring stations at high-, middle-, and low latitudes in the American, European/African, and Asian/Australian sectors. Solar, solar wind, interplanetary, and geomagnetic data were also obtained through the NOAA Space Environment Services Center. The period began with nearly two full days of typically quiescent solar minimum conditions, with the night of the 6th marking a transition to a substantial increase in solar wind velocities, and enhanced dynamics in the interplanetary magnetic field with associated geomagnetic disturbances. The increased solar wind velocities resulted from a corotating high-speed stream coupled to a transequatorial solar coronal hole. Evidence points to a step-wise coupling of processes from the coronal hole through the interplanetary and magnetospheric domains down to the equatorial ionosphere, where penetrating electric fields participated in triggering the most disturbed condition of equatorial spread-*F* ever recorded by the Jicamarca Observatory. The correlation of events also included : (1) enhanced particle precipitation power at high latitudes, (2) an associated cross polar cap potential of 75 kV, and (3) simultaneous global observations of *F*-region dynamics. In addition, detailed model comparisons with observations of the quiet and disturbed ionosphere point to requirements for improved global specification of thermospheric winds and electric fields. The content of this paper presents an overview of the program, its initial findings, recommendations, and future perspectives.

Annales Geophysicae, 1988, **6**, (1), 3-18.

1. BACKGROUND

Brief statement of the problem

The solar-terrestrial system is very complex, with a myriad of macro- and microphysical processes that challenge the development of a unified physical description that synthesizes the contributions of solar, magnetospheric, interplanetary, and ionospheric physics. A well-planned interdisciplinary effort combining theoretical modelling with a coordinated global-scale measurement program should lead to significant advances in our understanding of the solar-terrestrial system as a whole and the development of a real-time predictive capability for the ultimate interactions and subsystem responses in the entire Sun-Earth network.

The general approach of the SUNDIAL program is illustrated in figure 1, a schematic presentation of elements that focus on the ionosphere, but require solar and interplanetary inputs and a detailed understanding of the interactive roles that the ionosphere plays with the magnetosphere and the thermosphere.

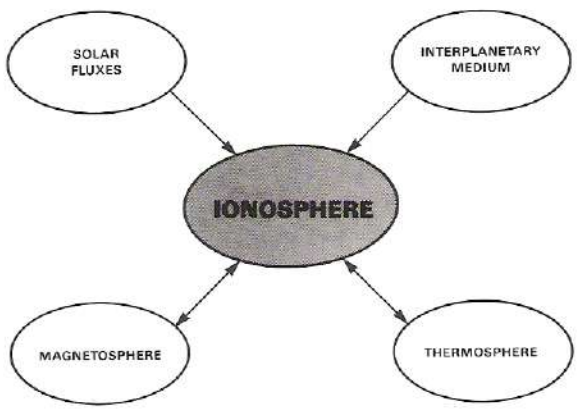

Figure 1
Schematic illustration of phenomenological domains covered in the SUNDIAL *objectives.*

The program couples global-scale theories and experiments as an *a priori* condition for the test and development of our understanding of contributing cause-effect relationships. The first experimental campaign employed nearly 70 ground-based ionospheric stations, most of them operating around-the-clock for the period 5-13 October, 1984. The ionospheric data were supplemented with solar and magnetogram information from the National Oceanographic and Atmospheric Association (NOAA), and the monitoring of the interplanetary medium was provided by the IMP-8 and ICE spacecraft. Theoretical models focussed on a first principles approach to global-scale ionospheric *F*-region processes, with a synergistic approach to magnetospheric and thermospheric modelling, and attendant interactions. From a purely empirical perspective, the IRI (International Reference Ionosphere (Rawer, 1981)) also played a role in the program objectives, inasmuch as it is a widely available description of *E*- and *F*-region parameters and oftentimes invoked as an accurate description of averaged solar, seasonal, and solar-cycle controls. The IRI and first principle codes are critically compared with accumulated global-scale data in the SUNDIAL investigation.

In the sections that follow, a general description of ionospheric processes will be advanced in order to establish a perspective on the active coupling networks involved in ionospheric predictions and to establish the general expanse of the problem being addressed. Specifics of the SUNDIAL investigation will then provide details on the measurement program, associated observations, and theoretical model descriptions. Commentary will also be advanced with regard to perspectives on future requirements and program plans.

The ionospheric domain and some coupling processes

An overview.

While the Earth's ionosphere is a major terrestrial sink for solar and magnetospheric events (Wolf, 1975, 1982 ; Fisk *et al.*, 1984), it is far from a passive element in the solar-terrestrial system, for the spatial distribution of ionospheric conductivity can affect magnetospheric plasma transport and the configuration of the magnetospheric current system (cf. Chiu *et al.*, 1984). Its interactive role is also evident from accumulating satellite measurements which show the ionosphere to be an important source of ions in the magnetosphere.

Within its own right the ionosphere is a complex subsystem having its own intrinsic coupling networks. Traditionally, ionospheric studies have been divided into phenomena at low-, middle-, and high geomagnetic latitudes where fundamentally different mechanisms can be associated with the degree of magnetic-field coupling to higher altitude magnetospheric events. At low latitudes, where the geomagnetic field tends to be horizontal, the coupling to the higher altitude magnetosphere is largely through indirect effects (wind systems, electrojet currents, travelling ionosphere disturbances (TID's), electric fields, etc.), while at high latitudes the more vertical magnetic field promotes strong magnetospheric coupling and direct access of energetic particles. To date, many of these elements have been studied separately, with no major attempts at a fully-integrated approach.

With regard to coupling and dynamics, the nighttime equatorial ionosphere has been intensively studied, particularly under conditions of equatorial spread-*F* (ESF) (Fejer and Kelley, 1980 ; Abdu *et al.*, 1983 ; Kelley *et al.*, 1982*a*, *b* ; Kelley and McClure, 1981 ; Keskinen *et al.*, 1981 ; Livingston *et al.*, 1981 ; Ossakow, 1981 ; Rino *et al.*, 1981 ; Tsunoda, 1985 ; Tsunoda *et al.*, 1982). The overall ESF process is a nighttime phenomenon (usually occurring within the period 2300 ± 300 h local time), centered about the magnetic equator in a belt about $\pm 20^{\circ}$ wide, with seasonal, solar-cycle, and day-to-day variations superimposed. The triggering of ESF is intimately related to flux-tube integrated conductivities, thermospheric winds, and global-scale electric fields, with the latter two terms having driving forces traceable to high latitudes and to dynamics in the interplanetary and magnetospheric domains.

Before proceeding with detailed discussions of global *F*-region dynamics and associated coupling processes, we introduce a general commentary on the *E*-region ionosphere (Szuszczewicz *et al.*, 1978 ; Farley *et al.*, 1978 ; Fejer and Kelley, 1980 ; Pfaff *et al.*, 1984). By contrast with the *F*-region, the *E*-region is less understood, largely because of its inaccessibility to systematic global investigations by satellites. The *E*-region must be probed with rockets, ground-based radar, and HF sounding systems. This has resulted in geographically-localized studies of *E*-region phenomena, which by their very nature are deficient in information on horizontal variations. While not considered of major importance when viewed from a perspective of total ionospheric electron content, the *E*-region can play an active interchange role with a number of *F*-region processes, and must therefore be reckoned with in the development of any comprehensive model attempting to treat (or predict) ionospheric plasma distributions and transport. In this context we note that the *E*-region plays a major role in global-scale current systems and electric fields.

Equatorial spread-F (ESF)

The problems of predicting the onset of processes leading to macro- and microscale ionospheric structure often depend on accurate descriptions of phenomena remote from the site under study. As an illustration, consider irregularity development during the occurrence of equatorial spread-*F*. Spread-*F* can, in first order, be thought of as a two-fluid instability process (heavy fluid resting on a light fluid supported by gravity), with the nighttime F_2-layer ($N_e \sim 10^6$ cm^{-3}) being the heavy fluid and the lower-density molecular-ion region directly below it ($N_e \sim 10^3$-10^4 cm^{-3}) being the light fluid. The system is supported against gravity by a horizontal magnetic field. Pushing the two-fluid analogy one step further, one can appreciate that a disturbance at the two-fluid interface (e.g., *via* electric fields or thermospheric winds) would result in a rising bubble with attendant breakdown to smaller structures.

The definition of ESF irregularities has advanced to a point where there is a reasonably good understanding of their scale size distributions, cause-effect relationships, and day/night, seasonal and solar-cycle variations (e.g. Bandyopadhyay and Aarons, 1970 ; Basu *et al.*, 1978 ; Costa and Kelley, 1978*a*, *b* ; Dyson *et al.*, 1974 ; Huba and Ossakow, 1979, 1981 ; Kelley *et al.*, 1982*a* ; Matsushita and Kamide, 1981*a*, *b* ; McClure *et al.*, 1977 ; Singh and Szuszczewicz, 1984 ; Szuszczewicz, 1978 ; Szuszczewicz *et al.*, 1980 ; Tsunoda, 1980 ; Tsunoda *et al.*, 1979). This does not mean that a truly-predictive capability is in hand, but rather that we have a substantially improved understanding of several connected processes. For example, in our understanding of ESF it is clear that the zero-order parameters of *F*-region height, bottomside gradient, and overall *F*-region rise velocity are important factors which optimize the probability for the onset of ESF. Accumulating theoretical and experimental results show that higher *F*-region altitudes, smaller bottomside gradient scale lengths, larger *F*-layer post-sunset rise velocities, and larger initial bottomside disturbances all enhance the probability of ESF occurrence. These are basic *F*-region parameters (with the exception of the « initial disturbance ») for which there is no accurate predictive capability. On any given night the appearance of ESF can only be « predicted » by relying on persistence or on statistical studies of seasonal and solar-cycle probabilities. This was dramatically demonstrated in the BIME (Brazilian Ionospheric Modification Experiment) Campaign when an attempt was made to trigger ESF through a man-made macroscale plasma structure created by chemical injection on a vertically-rising, steep, post-sunset, bottomside *F*-layer gradient (Narcisi, 1983 ; Szuszczewicz *et al.*, 1983).

With regard to controlling zero-order parameters, a long-standing dilemma has been the longitudinally-dependent seasonal variation of ESF. Tsunoda (1985) suggested that the seasonal maxima in ESF and associated radio wave scintillation activity (originally thought to coincide with the spring and autumnal equinoxes) coincide with the time of year when the solar terminator is most nearly aligned with the local geomagnetic flux tubes. He showed that ESF had the highest probability of occurrence when the flux-tube integrated *E*-region Pedersen conductivity was changing most rapidly... a situation that exists when conjugate *E*-region footprints of a given magnetic flux-tube undergo a near-simultaneous sunset. This interpre-

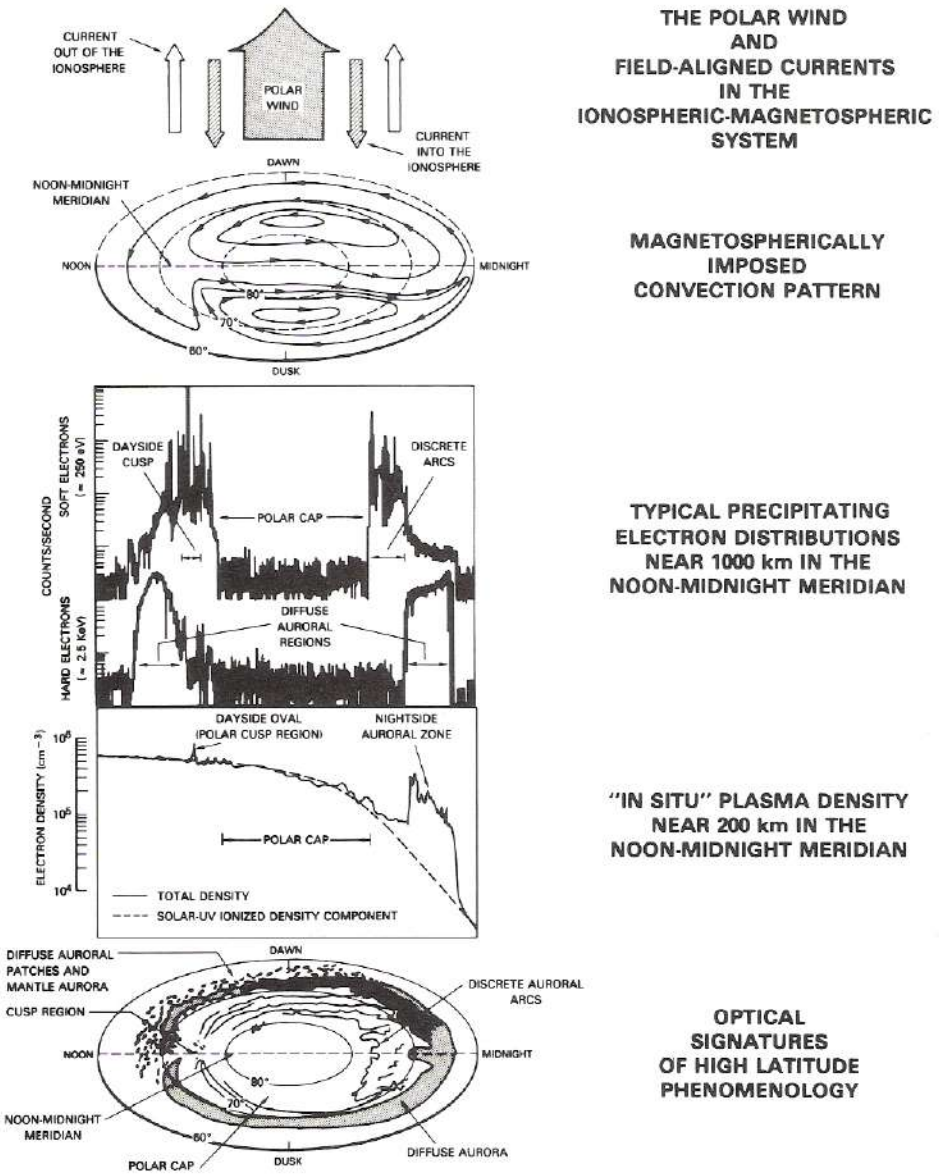

Figure 2

Composite illustration of high-latitude ionospheric processes : phenomenology, irregularity distributions, transport and magnetospheric coupling. The format is in coordinates of magnetic-local-time and magnetic latitude with specific adaptations from the works of Akasofu (1981) *and Szuszczewicz* (1984).

tation is consistent with equatorial irregularity generation by the collisional Rayleigh-Taylor instability and irregularity-growth enhancement by gradient drift instabilities. A somewhat parallel suggestion has come from analysis of topside soundings by the ISS-b satellite (Murayama and Matuura, 1984), with the conclusion that any effects based on the magnetic field configuration alone could not explain the longitudinal-seasonal variation of ESF. The investigators maintained that the neutral wind direction relative to the magnetic meridian was an important seasonal consideration that tended to match their data and accumulated statistics on global ESF distributions.

High-latitude considerations.

High-latitude ionospheric plasma populations are a culmination of processes that include EUV and energetic-particle ionization, ion chemistry, horizontal and field-aligned transport, gradient- and current-driven instabilities, acceleration processes, and additional mechanisms yet to be uncovered in unravelling the global-scale picture (see Fejer and Kelley, 1980 ; Schunk *et al.*, 1984 ; Ossakow *et al.*, 1984 ; Szuszczewicz, 1984).

While the high-latitude ionosphere is extremely complex, ground-based and satellite-borne optical diagnostics have contributed substantially to a synoptic perspective of associated morphologies and phenomenologies (see lowest panel of fig. 2) with major domains having been identified as diffuse auroras, discrete auroral arcs, the polar cap and the polar cusp (Akasofu, 1981 ; Clark and Raitt, 1976 ; Kelley *et al.*, 1982 ; Schunk *et al.*, 1976 ; Rodriguez and Szuszczewicz, 1984).

The electron precipitation at high-latitudes is variable in its energy distribution, horizontal extent, and temporal characteristics (see « Precipitating Electron » panel in fig. 2). As a result, it creates horizontal and vertical ionospheric plasma structure by virtue of its own spatial, temporal, and energy configuration.

Once created, local plasma structures are subjected to magnetic-field controls, a magnetospherically-imposed convection electric field, and interactions with superimposed current systems (see top panels of fig. 2). The electric field that convects ionospheric plasma is intimately connected with the global-scale current systems flowing between the ionosphere and the magnetosphere. The intensity and detailed structure of the electric fields and currents are determined mainly by characteristics of the entire magnetospheric-ionospheric electrical circuit and the direction of the interplanetary magnetic field. Along with the polar wind, the convection electric field and current systems represent the fundamental link between the interplanetary medium and the near-Earth ionosphere.

Coupling to the magnetosphere and the interplanetary medium.

That the high latitude ionosphere exhibits an effective coupling with the magnetosphere and the interplanetary medium is an accepted fact, with perhaps one of the best illustrations being substorm activity. A recent investigation of this type of coupling was conducted by Rodriguez *et al.* (1987) who correlated *in situ F*-region irregularity behavior in auroral oval expansions with the southward turning of the interplanetary magnetic field (IMF). Figure 3 presents data that show how solar wind, magnetospheric, and ionospheric parameters were correlated throughout the two-day period which they studied. The upper three panels show the interplanetary solar wind parameters, $-B_z V_{sw}$ (the east-west electric field), ε (the coupling function, (Perreault and Akasofu, 1978 ; Murayama, 1982 ; Akasofu, 1983 ; D'Angelo and Goertz, 1979)), IMF (magnitude of the interplanetary magnetic field), and θ_{Bz} (the angle of the IMF relative to the Earth's magnetic moment) derived from measurements on board the IMP-8 satellite. The coupling function is given by $\varepsilon = V_{sw} B^2 \sin^4 (\theta/2) L_0^2$, where B is the IMF magnitude, θ is the polar angle of B in the y-z plane, and L_0 is a constant ($\simeq 7 R_E$). ε is often used as an estimate of the electromagnetic power flux entering the magnetosphere, with geomagnetic substorms gen-

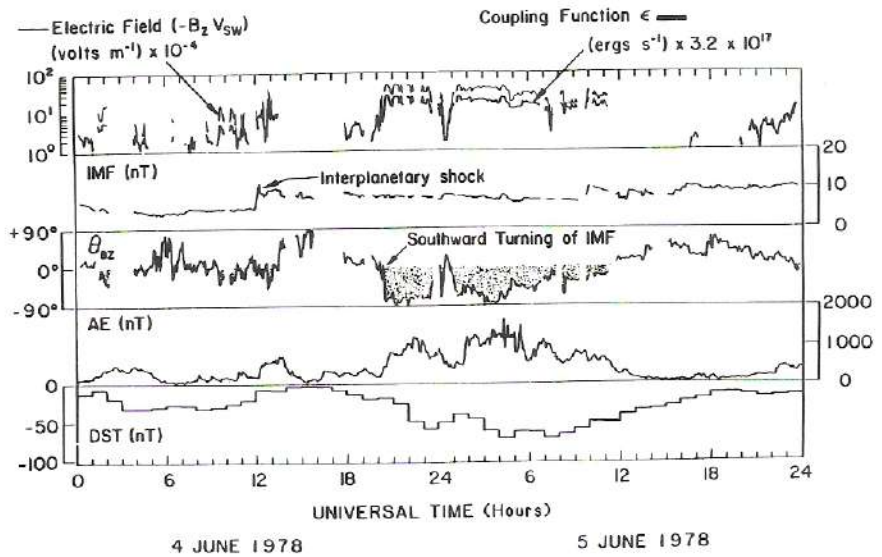

Figure 3
Correlations of activity indices which characterize the state of the solar wind and interplanetary magnetic field (upper three panels), the ionosphere and its current systems (fourth panel) and the magnetosphere (fifth panel). (From Rodriguez et al., 1987.)

erally associated with values of ε greater than about 10^{18} erg.s^{-1} (1 erg.s^{-1} = 10^{-7} watts).

Of special interest in figure 3 is the angle θ_{Bz} which defines the IMF vector with respect to the z-axis of the solar-magnetospheric coordinate system (direction of the Earth's magnetic moment). The condition of having a southward (negative z) component in the IMF is associated with an enhanced merging rate of the IMF with the magnetospheric magnetic field at the magnetopause and an increase in energy transfer to the magnetosphere (Russel, 1980). In contrast, a northward direction for the IMF correlates with subdued geomagnetic activity.

The fourth and fifth panels of figure 3 plot the *AE* and *Dst* indices, which are surface measurements of the perturbations (positive and negative) of the horizontal component of the geomagnetic field due to the auroral electrojet current and the magnetospheric ring current, respectively. Both *AE* and *Dst* are global disturbance indices obtained by synthesizing measurements from a network of ground stations situated around the world at the appropriate latitudes (Mayaud, 1980).

During the substorm duration studied by Rodriguez *et al.* (1987) the solar wind electric field and the coupling function ε were observed to track each other and correlate closely with θ_{Bz}. Variations in the *AE* and *Dst* indices also correlated with fluctuations in θ_{Bz}, but with a small lag. Throughout the substorm period, *in situ* plasma density measurements were collected by the S3-4 satellite (Szuszczewicz *et al.*, 1982) in the high-latitude *F*-region ionosphere in the altitude range 250-280 km. Correlation of ionospheric plasma irregularity intensities and their positions within the oval boundaries showed increased intensity and increased equatorward movement of the high latitude morphological domains (e.g. the nightside oval) with increasing *AE*. These results were not surprising but have been reviewed here to demonstrate the direct interplanetary-magnetospheric-ionospheric coupling and to highlight the uncertainty in predicting the southward turning of the IMF... a critical parameter in identifying the potential onset of a substorm and subsequent ionospheric dynamics. Like the vertical movement of the nighttime equatorial *F*-layer, θ_{Bz} can have dramatically unpredictable behavior (see fig. 3), with equivalent levels of unpredictability in the high-latitude ionosphere and the global electric field.

2. THE INTEGRATED APPROACH OF SUNDIAL

The ground-based program

To advance our fundamental understanding of ionospheric controls and improve global-scale prediction capabilities, the SUNDIAL program has combined theory with measurement in a stepwise progressive investigation covering seasonal and solar cycle variations.

The SUNDIAL ionospheric monitoring network includes high-, middle-, and low latitudes in the American, European/African and Asian/Australian sectors (see fig. 4) with an agreement on common data formats and around-the-clock data collection. The first SUNDIAL campaign covered a contiguous 8-day period from 5-13 October 1984, with solar, solar wind, interplanetary, and geomagnetic data provided through the National Oceanographic and Atmospheric Association (NOAA).

The ground-based ionospheric measurement techniques included ionosondes, backscatter radars, VHF polarimeters, scintillation receivers and all-sky and scanning photometers. Ionosonde measurements were made at least every hour, and normally once every 15 min for the entire eight-day period.

While stations agreed on a uniform plot format for geophysical parameters, the backscatter radar formats in the SUNDIAL program were simple adaptations of those which tend to be unique to a given facility. In addition, radar observation time was substantially less than that of other ground-based diagnostics, primarily because of associated costs.

The scanning 6300 Å photometers were incorporated to provide meridional and/or zonal profiles of airglow intensity. These measurements were designed to provide information on E-W, N-S distributions of large-scale ionospheric features and their temporal evolution. Typically, meridional and zonal scans were operated at a rate of one scan per minute covering an angular variation of ± 75° from vertical and repeated hourly throughout nighttime portions of the eight-day campaign.

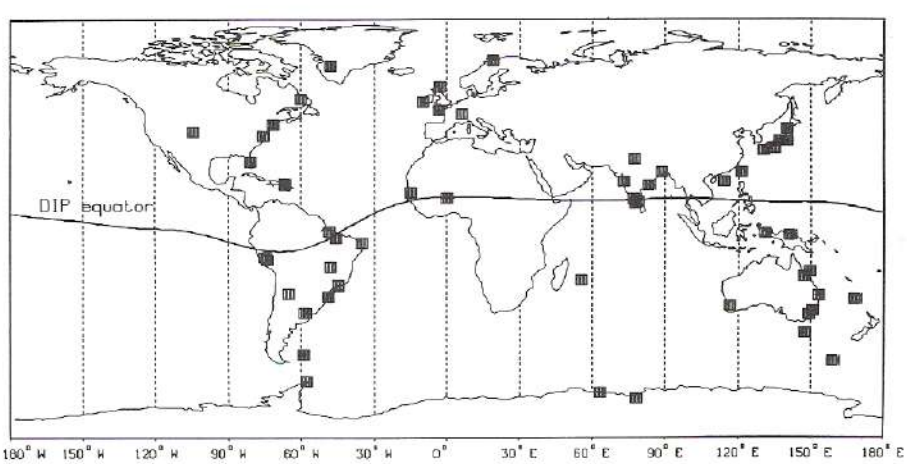

Figure 4
Global network of SUNDIAL *ground stations.*

The modelling program

An overall perspective on requirements.

The overall goal of the SUNDIAL program is the development of a predictive capability for the condition of the ionosphere in its quiescent and disturbed states. In reducing this statement to its most fundamental definition, the goal requires the prediction of the ionospheric plasma density profile $N_e(z)$ at all latitudes and longitudes. Time dependence is of course implicit. Accordingly, the accurate specification of $N_e(\mathbf{r}, t)$, with relevant parameter definitions illustrated in figure 5, is shown as the final output in the simple flow diagram of the measurement and modelling activities in the program (see fig. 6).

The zeroth-order input requirements (left-most box in fig. 6) trace themselves to the Sun, but require only definition of the interplanetary parameters involving the solar wind density and velocity, and the interplanetary magnetic field and its vector direction. Coupling these primary input terms to the required output are first principle codes (discussed below) which treat the magnetospheric, thermospheric, and ionospheric domains. The codes are not « first principle » from a purist's perspective, for they require a number of empirical model inputs to couple themselves to processes that go beyond the current capabilities for a full-scale self-consistent « first-principles » approach. This, however, is considered a realistic starting point for establishing the predictive properties of the system.

The magnetospheric model.

The ultimate program requirement on a magnetospheric model is the accurate prediction of precipitating particle fluxes and magnetospherically-imposed ionospheric electric fields. Looking to the left-most block in the program flow diagram (fig. 6), the primary input requirements are the three fundamental parameters of the interplanetary medium $(\rho, v, B_{\mathrm{IMF}})$. Code requirements, however, necessitate the additional input of a number of empirical

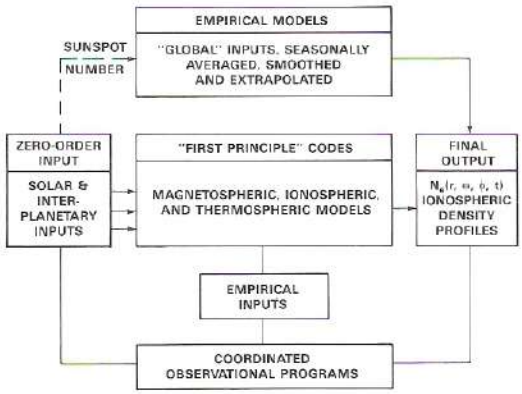

Figure 6
The modelling and measurement approach of the SUNDIAL *program.*

model specifications. In an ideal situation this requirement is limited to the empirical definition of the field-line integrated conductivities $\left(\int \mathrm{d}\ell\ \underline{\underline{\sigma}}\right)$ and the weighted integral of wind velocity

$$\left(\int \mathrm{d}\ell\ \underline{\underline{\sigma}} \cdot (\mathbf{v}_n \times \mathbf{B})\right)$$

with E-region winds being most crucial. The baseline model is that generally referred to as the « Rice Convection Model » (Harel *et al.*, 1981*a*, *b*). It covers the lower latitude part of the auroral zone, beginning roughly at the equatorward edge of region-1 Birkeland currents, and extends out to about $10\,R_E$ in the equatorial plane. The required model inputs include :

1) the polar-cap potential drop (estimated from the IMF input) ;

2) the initial distribution of the magnetospheric plasma ;

3) the distribution function of plasma entering the modelled region ;

4) a model of the thermospheric winds ;

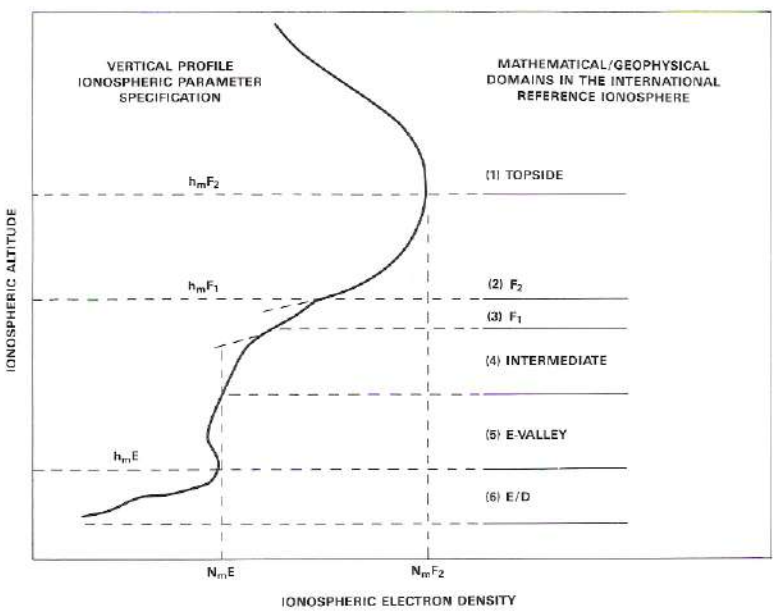

Figure 5
Ionospheric layer specifications and domains in the empirical prescription of the International Reference Ionosphere. SUNDIAL *efforts focus on the E- and F-regions.*

5) field-line integrated conductivities ; and

6) a magnetospheric magnetic field model (ρv^2 input).

The model provides a consistent picture of the plasma sheet, ring current, the plasmasphere and ionospheric-related parameters. The auroral electric field profiles tend to be more realistic than co-latitude power-law descriptions (e.g. Harel *et al.*, 1981*b*) and the model provides an improved representation of electric field penetration to low latitudes (Spiro *et al.*, 1981). Some of the newer features in the code (e.g., the thermospheric wind model) are being tested in the SUNDIAL program. Specific model outputs, detailed in the paper by Spiro *et al.* (1988), include :

1) ionospheric electric fields and horizontal currents ;

2) magnetospheric electric fields and currents, including magnetospheric field-aligned currents ;

3) magnetospheric particle distributions, including those in the plasma sheet and radiation belts, and

4) fluxes of precipitating electrons.

Items 1 and 4 represent the primary coupling terms that affect the specification of the global-scale ionosphere.

The ionospheric modelling approach.

The model adopted for test and development in the SUNDIAL program is that described by R. W. Schunk and co-workers (Schunk and Walker, 1973 ; Schunk *et al.*, 1975, 1976 ; Schunk and Raitt, 1980 ; Schunk and Sojka, 1982*a*). It is a time-dependent, 3-dimensional, multi-ion (NO^+, O_2^+, N_2^+, O^+, N^+, He^+) model of the global ionosphere at altitudes between 120 and 800 km. The model takes account of the effects of field-aligned diffusion, cross-field electrodynamic drifts both in the equatorial region and at high latitudes, interhemispheric flow, thermospheric winds, polar wind escape, energy-dependent chemical reactions, neutral composition changes, and ion production by EUV radiation and auroral precipitation.

Altitude profiles of the ion and electron temperatures and the six ion densities are obtained by solving the appropriate continuity, momentum, and energy equations. At middle and high latitudes, the equations are solved over the altitude range from 120 to 800 km, with chemical equilibrium at 120 km and a specified plasma escape flux at 800 km being the lower and upper boundary conditions, respectively. At low latitudes, the densities are computed along trans-equatorial flux tubes from 120 km in one hemisphere to 120 km in the conjugate hemisphere.

A number of parameters are required as inputs to this model. The ionization is produced through three mechanisms : EUV solar radiation, resonantly scattered radiation, and auroral precipitation. For each, the input source needs to be specified. Also, the neutral atmospheric composition and temperature are required ; for these the mass spectrometer/incoherent scatter (MSIS) model has been adopted (Hedin, 1983). In addition, both thermospheric wind and magnetospherically imposed convection electric-field patterns are needed.

To date, the ionospheric model has been used mainly to study high latitude phenomena. The focus of the high-latitude work has been the study of the ionospheric response to slow convection in winter (Sojka *et al.*, 1981*a*, *b*), rapid convection in winter (Sojka *et al.*, 1981*c*), and rapid convection in summer (Sojka *et al.*, 1982). The model was also used to study the ion temperature variation in the daytime high-latitude ionosphere for a wide range of conditions (Schunk and Sojka, 1982*a*), and it was used to uncover the presence of ion temperature hot spots during periods of sustained high magnetic activity (Schunk and Sojka, 1982*b*). More recently, the ionospheric response to « stormlike » variations in some of the important magnetospheric inputs, including the plasma convection pattern and the precipitating auroral electron flux (Sojka and Schunk, 1984, Sojka *et al.*, 1983), was studied. So far, only one attempt at a fully global study has been conducted (Sojka and Schunk, 1985*a*). The current investigation will provide a multiplicity of test points at the magnetospheric and ionospheric boundaries of the code. Papers by Abdu *et al.* (1988), Leitinger *et al.* (1988) and Wilkinson *et al.* (1988) treat a detailed comparison of the code with SUNDIAL observations and include an additional comparison with the empirically-derived International Reference Ionosphere (see also Schunk and Szuszczewicz, 1988).

The International Reference Ionosphere.

Empirical models are based on a statistical and/or numerical description of the ionosphere in terms of location (geographic or geomagnetic), time (solar zenith angle), solar activity (10.7 cm flux or sunspot number), and season. By definition, empirical ionospheric models are based on accumulated data, including critical frequencies ($f_0 E$, $f_0 E_s$, $f_0 F_1$, and $f_0 F_2$), altitudes of peak concentrations ($h_m E$, $h_m F_1$, and $h_m F_2$), and half thicknesses of the individual layers. The data is compiled typically from ionosondes, topside sounders, and *in situ* satellite and rocket profiles (wherever available). Averaged profiles are then synthesized, and analytical fits developed (fig. 5) with the end product representing an intelligent mix of empiricism, physics, extrapolation, and intuition. In many cases the quality of the empirical model representation of actual conditions is directly related to available data, its global distribution, parameter space converge, time base, and accuracy. Obvious gaps include ionogram definition of the *E-F* region valley, subionospheric locations over oceans, and *F*-region characteristics under condition of blanketing sporadic-*E*. By definition, averaged empirical profiles provide no information on irregularity structure, and accordingly are intrinsically inaccurate in those ionospheric domains where irregularity structures are the norm. One such domain is the high-latitude ionosphere where empirical models have major shortcomings and ionosonde data bases can be compromised in attempts to provide fundamental height profile information.

Notwithstanding the limitations imposed on empirical models, they can (and do) provide a valuable resource that includes a broad experience base in ionospheric profiling and data archiving. In addition, many empiri-

cal models (e.g., IRI, the International Reference Ionosphere) are made available internationally for applications to individual investigator interests. If the ultimate goal of the SUNDIAL program is to be realized, an interactive real-time modelling and data acquisition effort must evolve ; and requirements for minimum computational time will dictate a merger of concepts in long-running first-principles and shorter-form empirical codes.

There are a number of contemporary schemes for empirical modelling of ionospheric profiles, with reviews included in the works of Dandekar (1982) and Dudeney and Kressman (1986). After comparisons with synoptic satellite data and the empirical model of Chiu (1975), the International Reference Ionosphere (IRI) was selected as the best available empirical representation of the ionosphere, and was adapted for more intensive comparisons in the SUNDIAL investigations (Schunk and Szuszczewicz, 1988).

The IRI (Rawer, 1981 ; Schunk and Szuszczewicz, 1988) provides global-scale information not only on the macroscale features of electron density (as in fig. 5), but also on the ion and electron temperatures, and the ion composition. These additional features make the IRI an attractive model for comparison with SUNDIAL data and our first-principle code results. The IRI is an evolutionary code which makes no pretense about predictive capabilities, with its primary emphasis being an attempt at a global-scale representation of observations. In this regard the IRI makes its limitations clear, particularly with regard to the relative paucity of ion composition results. The founders and contributors to the IRI encourage workers in the field to help fill in the gaps, both in the understanding of ionospheric processes, and in the scope of experimental coverage. We expect that the SUNDIAL activities will be most useful in its theoretical and experimental comparisons with the IRI.

The IRI profiles are generated by a synthesis of functions descriptively identified with each of six different mathematically- and/or geophysically unique altitude regions (see right side of fig. 5). Exercise of the IRI software package requires external specification of date, time, position, and solar activity (sunspot number) ; and the outputs are tabular lists of N_e, T_e, T_i, and M_i. Intrinsic to the software package are the required input parameters discussed above. The details of IRI products relevant to the SUNDIAL measurement and modelling program are presented in a series of papers (Schunk and Szuszczewicz, 1988 ; Wilkinson *et al.*, 1988 ; Abdu *et al.*, 1988 ; Leitinger *et al.*, 1988).

3. AN OVERVIEW ON OBSERVATIONS AND ANALYSES

Solar, interplanetary, and geomagnetic conditions

Solar and interplanetary.

The first SUNDIAL campaign was conducted in October 1984, approaching solar minimum in the declining phase of Solar Cycle 21 (see fig. 7). The year 1984 may be related to 1973 of Solar Cycle 20, and to 1962 of Solar Cycle 19, noting that the true

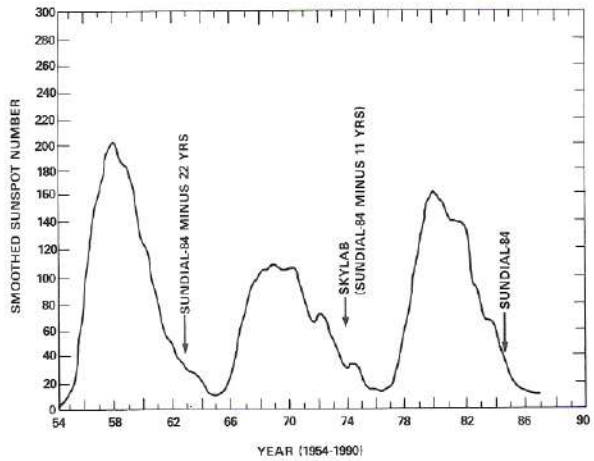

Figure 7
Sunspot numbers for Solar Cycles 19-21, *showing* SUNDIAL-84 *period and previous solar cycle correlation with* SKYLAB.

period of solar activity is 22 years (in association with a double reversal of polarities) and that geomagnetic activity is more similar in 22 year correlations, particularly in the declining phase of solar activity.

The October 1984 SUNDIAL period fell within an essentially flare-free interval that included the rise, maximum, and fall in the velocities of a co-rotating high-speed solar wind stream that was associated with the equatorward extension of a polar coronal hole. With the exception of the transition to the dynamics associated with the high-speed stream, solar phenomenology was nominally that of a typical solar minimum condition. Solar activity was very low throughout the SUNDIAL period with the Sun spotless for several days. The 2800 MHz (10 cm) solar flux measured at the Ottawa Radio Observatory was 74 ± 1 flux units, (see top panel of fig. 11) only a few units above the levels seen during the previous solar minimum. There were no significant flares at soft-X-ray wavelengths (1-8 Å), or notable solar radio noise events during the period ; and only a few optical flares were reported with no significant enhancements in energetic particle fluxes measured at geosynchronous satellite altitudes (GOES data, J. Joselyn, private communication).

The interplanetary observation of the high-speed solar wind stream shown in figure 8 bore the classic characteristics of high speed and low densities. Fig-

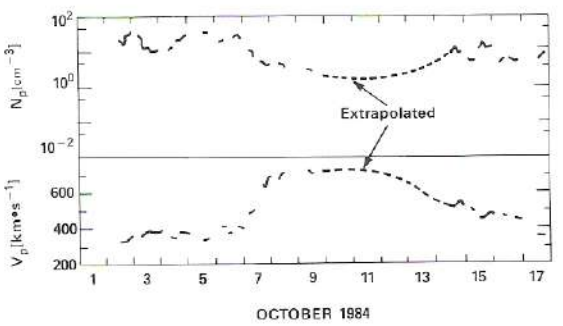

Figure 8
Smoothed 1-h *averaged solar wind parameters of density and bulk velocity as measured by the* MIT *plasma instrument on the* IMP-8 *spacecraft (courtesy I. Lazarus). Dotted curve is an extrapolation of results.*

ure 9 presents the complementary but fragmentary IMF B_z data that were accumulated by the IMP-8 spacecraft. The source of the high-speed stream has been identified as the equatorward extension of the northern, solar, polar coronal hole seen in the middle and lower panels of figure 10. The northern hole, predominantly negative in magnetic polarity, extended across the Sun's equator with essentially meridional eastern and western edges. It was this north-south orientation of the hole's equatorial boundaries that gave the associated co-rotating high-speed solar wind stream its well-defined interplanetary structure (see figs. 8 and 10).

The class of streams associated with trans-equatorial coronal holes was first identified unambiguously, using coronal hole images and two spacecraft, by Krieger *et al.* (1973), and later confirmed by Nolte *et al.* (1976) in their analysis of Skylab data (see fig. 7 for solar cycle correlations). It is not surprising that the SUNDIAL stream resembles those during Skylab, since the much-studied Skylab streams were observed 11 years prior to SUNDIAL, during the declining phase of the previous Solar Cycle 20.

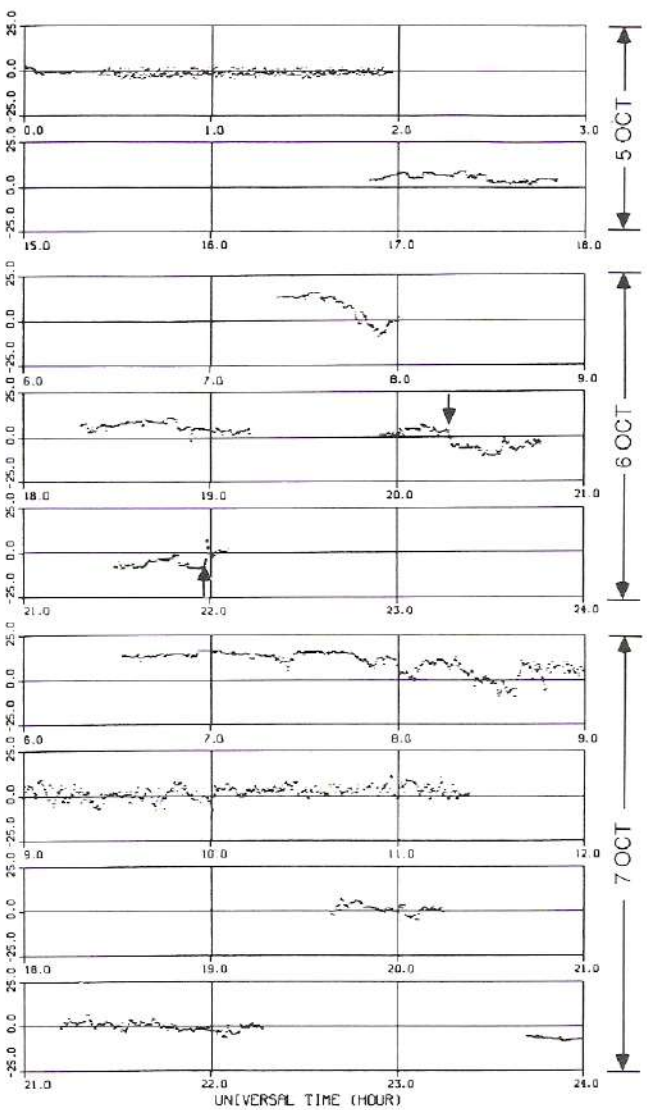

Figure 9

B_z-component of the IMF *for all measurement periods of the* IMP-8 *spacecraft on* 5, 6, *and* 7 *October* 1984 (*Courtesy of the* GSFC Data Center). *B_z units in* nT.

Geomagnetic conditions.

The trans-equatorial coronal hole and the associated interplanetary particle and magnetic field dynamics provided the causal terms for magnetospheric and ionospheric disturbances observed at the end of the second day in the SUNDIAL-84 campaign. The geomagnetic field was mostly quiet on the 5th and 6th ($A_p = 7$ on the 5th) and throughout the major portion of the SUNDIAL observation period. Exceptions include the 7th and 12th ($A_p = 43$ and 32, respectively), which pointed to storm-level disturbances (see fig. 11).

On the whole, the level of geomagnetic disturbance was typical of the generally active conditions experienced during the equinox periods of March-April and September-October each year. This annual average seasonal variation in geomagnetic activity (minima occur near the solstices) is not well understood, although various explanations have been proposed (Green, 1984). Figure 11 includes a comparison of the observed and forecast values for the Fredericksburg daily A-index and the GWC (Global Weather Central) A_p index. The agreement between predictions and observations is seen to be somewhat tenuous.

Ionospheric input power and responses

Analyses of high-latitude magnetograms (see Spiro *et al.*, 1988) support the existence of quiescent ionospheric and magnetospheric conditions at SUNDIAL times prior to 2000 UT on 6 October. The period 2000-2100 UT marked the onset of a substantial substorm with full development at 2200 UT (600 maximum excursion). This onset is reflected in the southward turning of the IMF at 2018 UT on 6 October and in the *Dst* and *AE* indices plotted for 6-7 October 1984 in figure 12 (adapted from Spiro *et al.*, 1988). Several of the magnetogram sites indicated the beginning of a recovery phase at about 2220 UT (see e.g. equatorial magnetograms in fig. 15) and at 2300 UT all stations had recovered. These results are consistent with the IMF data in figure 9, which show a southward turning of the IMF at 2018 UT on the 6th, with a sudden northward reversal at 2200 UT. The magnetogram results and attendant *AE* indices (see Spiro *et al.*, 1988) also suggest that the IMF maintained its northward orientation throughout the rest of the evening on the 6th (filling in the gap in the IMP-8 data). Magnetogram analysis also points to another substorm in the period 0100-0200 UT on the 7th.

A measure of energetic particle precipitation power at high latitude and the cross polar cap potential throughout the entire SUNDIAL period was made available through the NOAA/TIROS « precipitation activity index » (Foster *et al.*, 1986). The SUNDIAL-84 results are presented in figure 13, with an inspection of the results showing a correlation with the events described on 5 through 7 October. The figure also shows for that period a sustained precipitation power greater than 70 GW and a cross-polar cap potential averaging about 75 kV. These levels of power and potential correspond to a precipitation activity index 8 to 9 and an average K_p between 4° and 5⁻. Further inspection of figure 13 shows the low input power

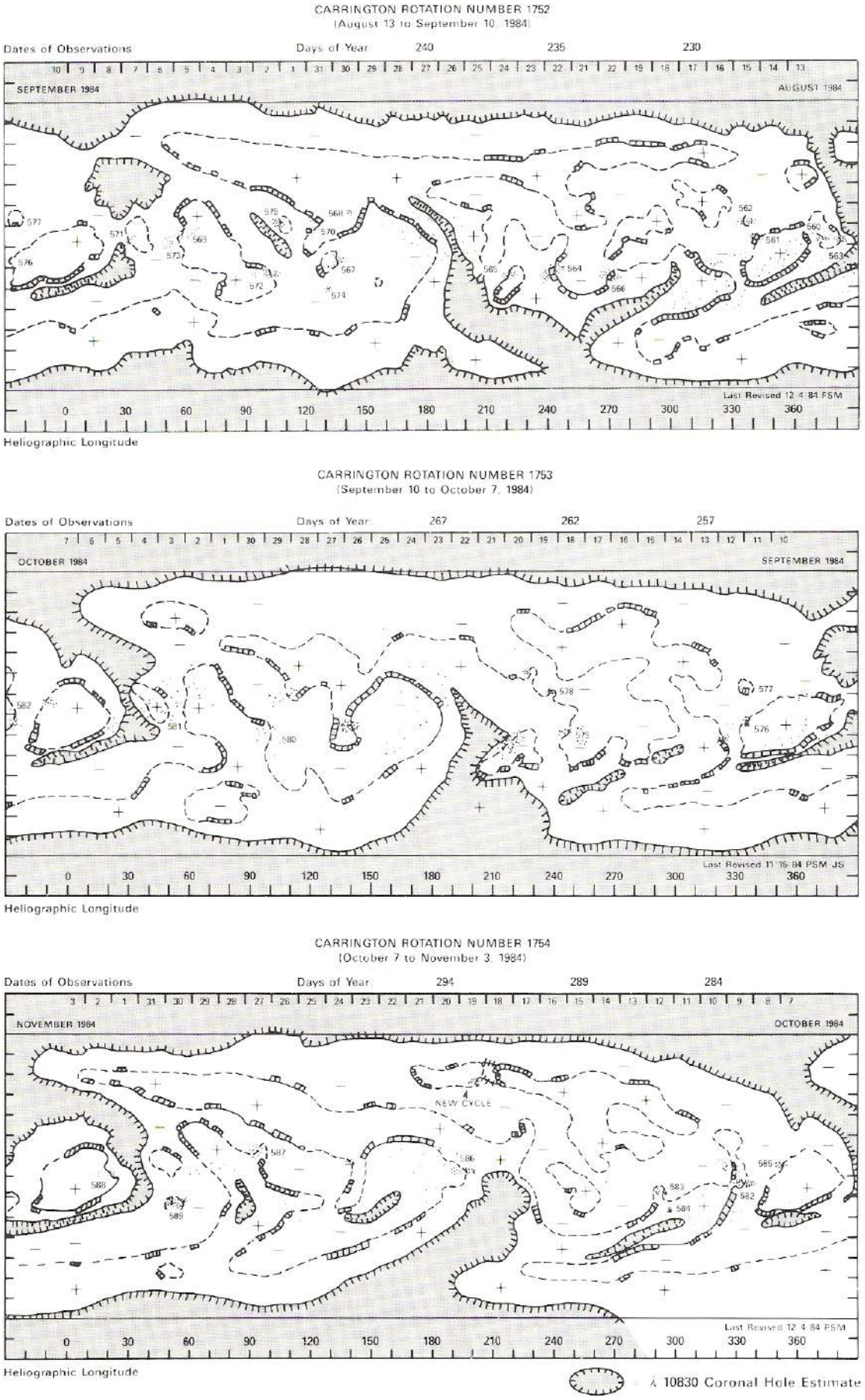

Figure 10

H-alpha synoptic charts of the solar surface for 27 day periods before (upper panel), during (middle panel), and immediately after (lower panel) the SUNDIAL-84 *campaign. The trans-equatorial, polar, coronal hole responsible for the high speed solar wind stream is depicted in the middle panel, centered about 4-5 October.*

levels on 5 October and through 20 UT on 6 October, and again in the final two days, 12-13 October, of the campaign.

SUNDIAL monitoring stations in the low-to-equatorial latitude zones registered ionospheric responses indicative of global-scale coupling to the interplanetary and magnetospheric disturbances. In the European sector the strongest mid-latitude disturbance occurred on October 8 (see Leitinger *et al.*, 1988), while at the equator in the South American sector intense spread-*F* conditions existed on the 6th through the 8th, with the 6th having recorded the most intense observation of equatorial spread-*F* ever documented by the Jicamarca Observatory (fig. 14). Global scale processes were clearly evident in the equatorial data which showed simultaneous *h' F* events in Brazil, Peru, Africa, and Southeast Asia (Abdu *et al.*, 1988).

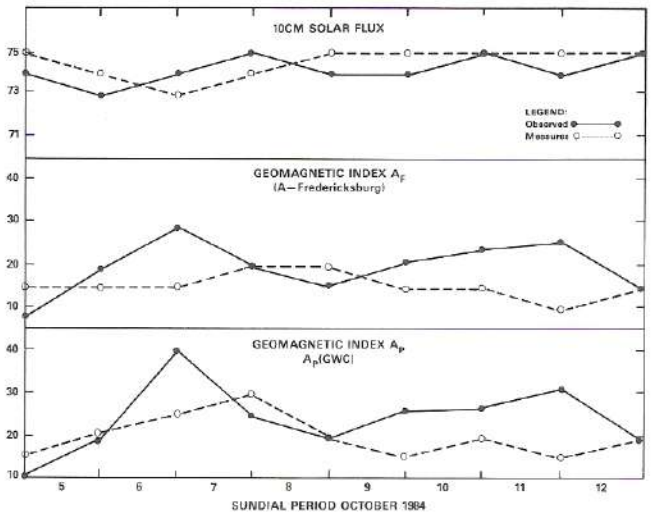

Figure 11

Predicted (dotted line) and observed (thick line) values of 10 cm *solar flux, and the Fredricksburg and planetary geomagnetic indices, A_f and A_p respectively.*

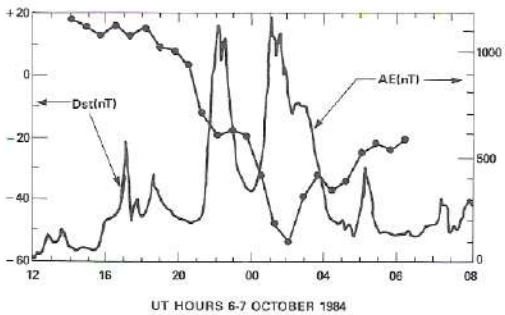

Figure 12

Dst and AE indices for 6-7 *October* 1984 *(adapted from paper by Spiro* et al., 1988).

The « record setting » spread-*F* and associated 3 m irregularity plume events at the Jicamarca Radar Observatory (fig. 14) followed a rapid increase in the vertical *F*-region plasma drift velocity that had its onset at about 1900 LT (see Spiro *et al.*, 1988). This vertical drift velocity enhancement, at a universal time of 00 UT on 7 October, is typical of low latitude electric field penetration events during magnetospheric disturbances. Such events in the dusk sector are often associated with sudden increases in magnetospheric convection (see Fejer, 1986 and Spiro *et al.*, 1988). Its occurrence, immediately following the normal evening *F*-region dynamo-induced pre-reversal enhancement in the vertical ionization drift (that had an onset at 18 LT (23 UT) on this day), is believed responsible for the intense nature of this unprecedented spread-*F* event over Jicamarca (see Fejer, 1981 ; Abdu *et al.*, 1988 ; Spiro *et al.*, 1988). Simultaneous fluctuations in *F*-layer heights and horizontal (*H*) components in magnetograms were observed at locations in the American, African, Indian, and Southeast Asian sectors of the equatorial zone. Evidence of coupling of the different ionospheric height domains was also detected at a number of geographic regions as well as on a global scale (Abdu *et al.*, 1988).

Figure 15 shows the *H*-component variations over Vassouras ($-28°$ dip), Brazil, and Huancayo ($-1°$ dip), Peru. The figure also presents *h' F*, $h_p F_2$, $h'_3 F$ variations, and the SUNDIAL spread-*F* index code (numbers 1, 2, and 3 depicting at any frequency the degree of spreading in the ionogram for thicknesses ≤ 100 km, 100-200 km, and > 200 km respectively). During this event simultaneous disturbances of the *H*-field were observed in the dayside hemisphere at Thumba ($\sim 1°$ dip), India. The global

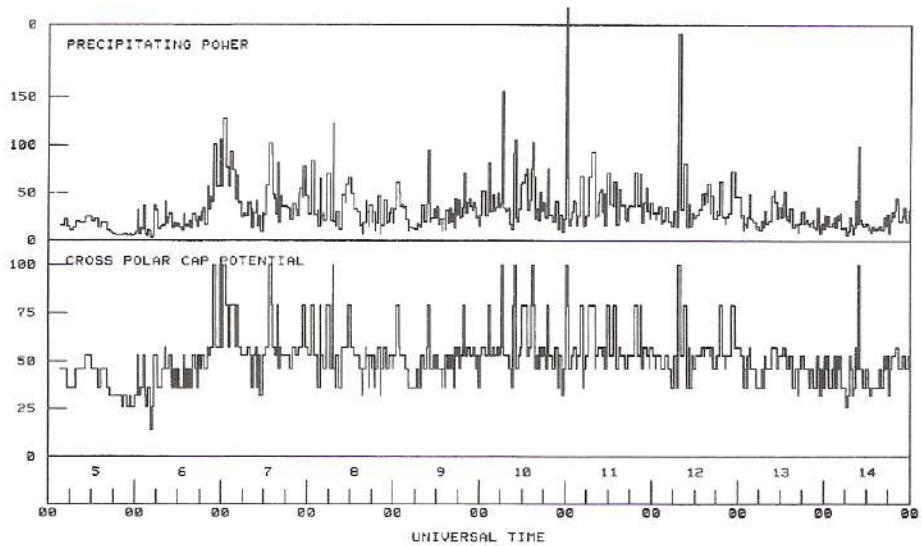

Figure 13

Energetic particle precipitation power at high latitudes and the cross polar-cap potential for the SUNDIAL-84 *period as calculated from* NOAA/TIROS *satellite data (Courtesy of J. Foster, see e.g. Foster* et al., 1986).

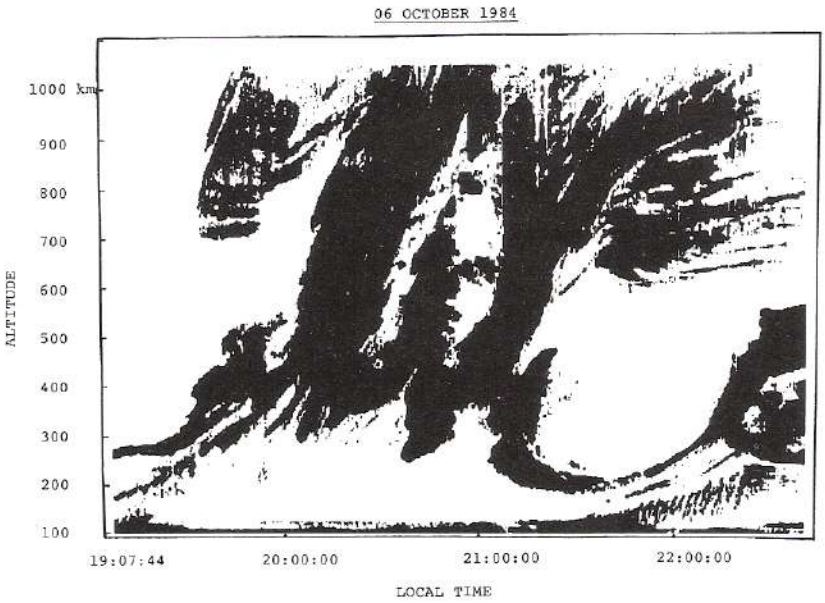

Figure 14
Jicamarca radar plot of reflected energy from domains of 3-m *plasma irregularities during the equatorial spread-F event of* 6-7 *October* 1984 (UT = LT + 5 h).

nature of magnetic field variations and the correlated *F*-region height changes over Cachoeira-Paulista suggest disturbed magnetospheric electric field penetration to the world-wide low-latitude ionosphere. This is corroborated by the Jicamarca radar data. The onset time of the electric field enhancement over Jicamarca at around 1845 LT (2345 UT) is also indicated in figure 15 by an arrow. During this disturbance, height variations at the same UT were observed in Africa, India, and Southeast Asia.

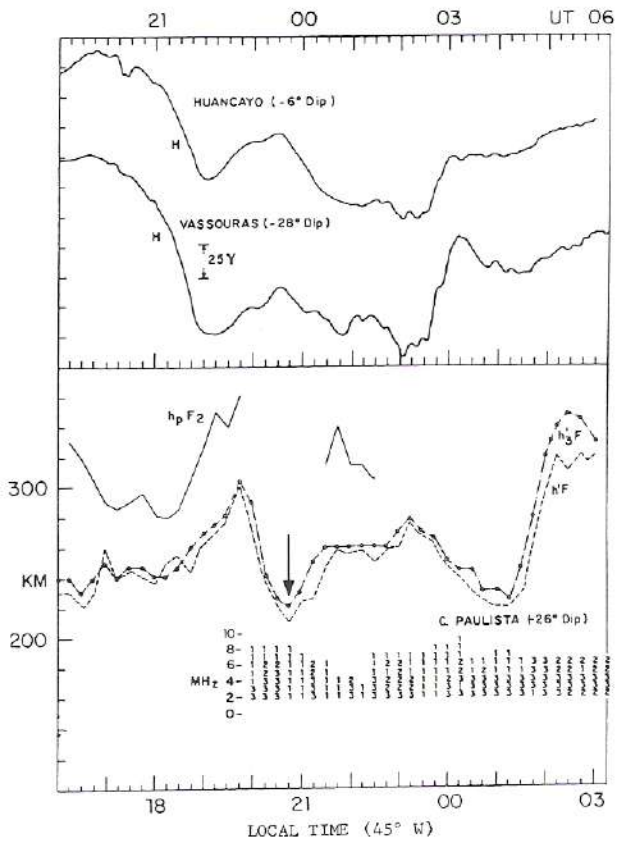

Figure 15
H-component magnetograms at Huancayo (Peru) and Vassouras (Brazil), and ionosonde data (including the SUNDIAL *spread-F index) for the F-region ionosphere above C. Paulista (Brazil), for* 6-7 *October* 1984. (UT = LT + 3 h).

Further evidence for the penetration of increased electric fields to low latitudes (resulting from the onset of events on the night of the 6th) is presented in figure 16, where real-height profiles (derived from ionosonde data) of ionospheric densities show increased *F*-region heights with each day following the most quiet period on the 6th. The figure also includes the very first comparisons of observations with the first principle code developed by Schunk and co-workers and with the International Reference Ionosphere (Rawer, 1981). The IRI output corresponds to the Ahmedabad station under conditions of low sunspot number in the seasonally-averaged October time frame.

On the first principle code results in figure 16 (and 17), it should be noted that the code output is sensitive at mid-latitudes to the adopted thermospheric wind pattern, with this test having considered only the meridional component. The wind model prescribed a maximum value of 200 m/s at night and a

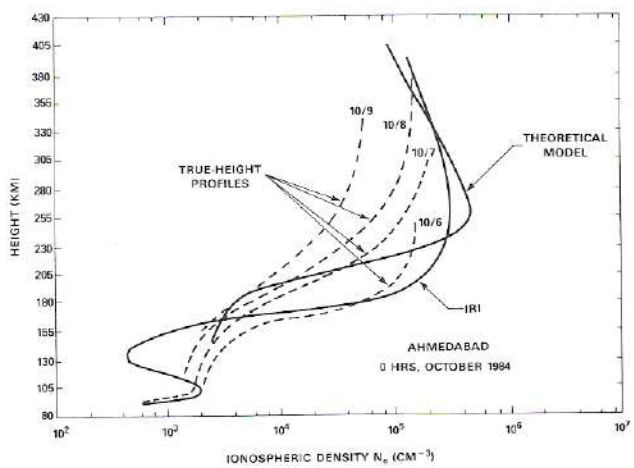

Figure 16
Comparison of observed ionospheric height profiles at Ahmedabad, India with the « predictions » of the International Reference Ionosphere (IRI) *and the theoretical model of Schunk and co-workers. The model calculations are intended to represent the undisturbed ionosphere observed on* 6 *October.*

minimum of 0 m/s during the day. Associated variations with latitude and longitude are described in Sojka and Schunk (1985*b*). At equatorial latitudes the model predictions are sensitive to the adopted equatorial electric field, with this preliminary test employing the quiet-time model of Richmond *et al.* (1980). Comparing the first-principle and empirical model outputs with the appropriate quiet-day conditions of 6 October favors agreement with the IRI in terms of the locations of the bottom-side gradient and the *F*-peak. Both models predict $N_m F_2$ values 2-3 times larger than observed. Substantially more comparisons are made in the papers of Wilkinson *et al.* (1988) and Abdu *et al.* (1988) with associated analyses and recommendations for model refinements.

An enlightening comparison of first-principle code results with observations at Ahmedabad is presented in figure 17, where a 24-h plot compares observations and predictions of $f_0 F_2$ and $h_m F_2$. The comparison shows a relatively good agreement in peak daytime values of both parameters but a substantial offset in the time at which the peaks occur. This initial finding points to the inadequacy of the empirically-derived electric field model (a fundamental input to the first principle code) and the requirement for its refinement and more global-scale testing. These efforts and associated effects on model predictions are reported on in the paper of Schunk and Szuszczewicz (1988).

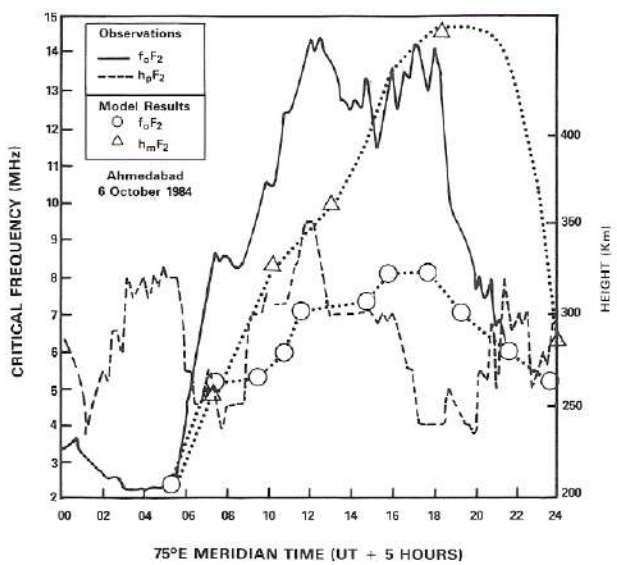

Figure 17

A 24 h *comparison of observed values for* $f_0 F_2$ *(critical frequency corresponding to* $N_m F_2$*) and* $h_m F_2$ *at Ahmedabad, India with the theoretical model prediction of Schunk and co-workers.*

4. COMMENTS AND CONCLUSIONS

The SUNDIAL-84 observations covered quiet and disturbed conditions, including the passage across the Earth of a well-defined, co-rotating, high-speed, solar-wind stream, unperturbed by solar flare activity. This provided a tremendous simplification in identifying cause-effect relationships, and allows some confidence that the results of SUNDIAL-84 analyses can be applied to other ionospheric disturbances associated with recurrent solar wind streams and dynamics in the IMF. Of course, the effectiveness of a high-speed stream to trigger a major magnetic storm depends to a large extent on whether the magnetosphere experiences extended periods of southward IMF. The generalization of our results to more complex solar wind structures must be cautious, but the first campaign has laid out the baseline phenomenology. Future campaigns will focus on a systematic study of « seasonal » ionospheric behaviors as we pass through solar minimum into the ascending phase of Solar Cycle 22. Figure 18 presents the SUNDIAL campaign schedule through 1991, with the development of coordinated global-scale neutral wind measurements, incorporation of the thermospheric NCAR/TGCM (see e.g. Fessen *et al.*, 1986) model, and intimate participation of satellite programs of opportunity (as of this writing the VIKING satellite and ground-based observational programs (Viking Science Team, 1986) have participated in the September/October 1986 and June 1987 investigations).

In SUNDIAL-84, measurements and models pointed to a coupling of processes involving a solar coronal hole, an associated high-speed solar wind stream, dynamics of the interplanetary magnetic field, and magnetospheric-ionospheric coupling to the equatorial ionosphere, where penetrating electric fields participated in triggering the most disturbed condition of equatorial spread-*F* ever recorded by the Jicamarca Observatory. The correlation of events also included

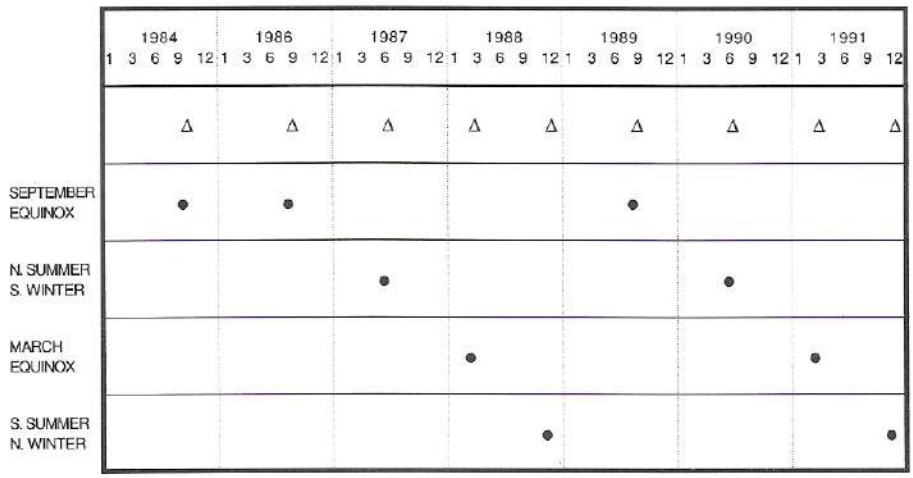

Figure 18

SUNDIAL *campaign schedule up to and including the maximum of Solar Cycle* 22. *Each campaign involves a minimum of* 8*-days of continuous ionosphere observations. The campaign of September* 1986 *was* 14 *days in duration and included the eclipse of* 3 *October* 1986.

sustained high-latitude energetic particle precipitation power greater than 70 GW ($4^{\circ} \leq K_p \leq 5^{-}$) and an associated cross polar potential about 75 kV ; and the global nature of the coupling processes was documented by simultaneous observations of *F*-region dynamics at the American, African, Indian, and Southeast Asian stations in the SUNDIAL network. Under the quiet-time conditions of the first two days of the campaign, comparisons of ionospheric data with the empirical models of Chiu and the International Reference Ionosphere (IRI) favor the IRI (Schunk and Szuszczewicz, 1988) while similar comparisons with the global-scale ionospheric model of Schunk and co-workers pointing to requirements for an improved specification of low-to-equatorial electric fields and global-scale thermospheric winds.

As we look forward to follow-on campaigns, the decline of Solar Cycle 21 continues into its minimum of activity (see fig. 7). The years 1984-1986 may be compared with 1973-1975 of Solar Cycle 20 (although a closer correspondence would be to 1962-1964 of Solar Cycle 19 as discussed earlier).

Solar and interplanetary observations in the previous solar cycle can provide a useful perspective on upcoming conditions. During 1973-1975, the interplanetary medium was dominated by two large high-speed solar wind streams, one from the north polar coronal hole and the other from the southern hole. However, by the end of 1975 (1986 for SUNDIAL), these large streams narrowed down and essentially vanished from the ecliptic plane because the equatorward boundaries of the holes were receding toward the polar regions.

By early 1976 (solar minimum), the stream structure was weaker and the persistence was only a few rotations. Thus, solar wind disturbances in 1987 would be less geoeffective and, more importantly, less predictable than the recurrent stream of SUNDIAL-84. Solar flare activity will also be minimal, so the 1986-1987 campaigns may well be truly « quiet-time » ionospheric studies.

Acknowledgements

This work has been supported by the National Science Foundation (NSF) under Grant No. ATM-8513362. To the NSF and to all participating countries and institutions, the SUNDIAL team extends its sincere thanks for dedicated support to this international endeavor.

REFERENCES

Abdu, M. A., R. T. de Medeiros, J. H. Sobral, and J. A. Bittencourt, Spread-*F* plasma bubble vertical rise velocities determined from spaced ionosonde observations, *J. Geophys. Res.*, **88**, 9197-9204, 1983.

Abdu, M. A., B. M. Reddy, G. O. Walker, R. Hanbaba, J. H. A. Sobral, B. G. Fejer, R. F. Woodman, R. W. Schunk, and E. P. Szuszczewicz, Processes in the quiet and disturbed high-latitude ionosphere : SUNDIAL campaign 1984, *Ann. Geophysicae*, **6**, 69-80, 1988.

Akasofu, S.-I., Auroral arcs and auroral potential structure, in *Physics of Auroral Arc Formation*, S.-I. Akasofu and J. R. Kan, (eds.), *Geophys. Monograph*, **25**, AGU, Washington, D.C., 1-14, 1981.

Akasofu, S.-I., Solar wind-magnetosphere energy coupling, in *High Latitude Space Plasma Physics*, B. Hultqvist and T. Hagfors (eds.), Plenum Press, New York, 1983.

Bandyopadhyay, P., and J. Aarons, The equatorial *F*-layer irregularity extent as observed from Huancayo, Peru, (Equatorial *F*-layer irregularity extent from propagation path observations to synchronous satellites), *Radio Sci.*, **5**, 931-938, 1970.

Basu, S., S. Basu, and B. K. Khan, Model of equatorial scintillations from *in situ* measurements (based on OGO-6 observed *F*-region irregularity), *Radio Sci.*, **11**, 821-832, 1976.

Basu, S., S. Basu, J. Aarons, J. P. McClure, and M. D. Cousins, On the coexistence of kilometer- and meter-scale irregularities in the nighttime equatorial *F*-region, *J. Geophys. Res.*, **83**, 4219-4226, 1978.

Chiu, Y. T., An improved phenomenological model of ionospheric density, *J. Atmos. Terr. Phys.*, **37**, 1563-1570, 1975.

Chiu, Y. T., R. Anderson, J. Fennell, L. Frank, R. Hoffman, M. Hudson, L. Lyons, P. Palmadesso, E. Ungstrup, R. Vondrack, D. Williams, and R. Wolf, Chap. 7 in *Solar-Terrestrial-Physics : Present and Future*, D. M. Butler, and K. Papadopoulous (eds.), *NASA Ref. Publ. 1120*, Washington, D.C., 1984.

Clark, D. H., and W. J. Raitt, Global morphology of irregularities in topside ionosphere, as measured by total ion current probe on ESRO-4, *Planet. Space Sci.*, **24**, 873-881, 1976.

Costa, E., and M. C. Kelley, On the role of steepened structures and drift waves in equatorial spread-*F*, *J. Geophys. Res.*, **83**, 4359-4364, 1978*a*.

Costa, E., and M. C. Kelley, Linear theory for the collisionless drift wave instability with wavelengths near the ion gyroradius, *J. Geophys. Res.*, **83**, 4365-4368, 1978*b*.

D'Angelo, N., and C. K. Goertz, An interpretation of Akasofu's substorm parameter, *Planet. Space Sci.*, **27**, 1015-1018, 1979.

Dandekar, B. S., Ionospheric modeling, AFGL-TR82-0024 Report, January 27, 1982.

Dudeney, J. R., and R. I. Kressman, Empirical models of electron concentration of the ionosphere and their value for radio communication purposes, *Radio Sci.*, **21**, 319-330, 1986.

Dyson, P. L., J. P. McClure, and W. B. Hanson, *In situ* measurements of the spectral characteristics of *F*-region ionospheric irregularities, *J. Geophys. Res.*, **79**, 1497-1502, 1974.

Farley, D. T., B. G. Fejer, and B. B. Balsley, Radar observations of two-dimensional turbulence in the equatorial electrojet, 3. Nighttime observations 9 type 1 waves, *J. Geophys. Res.*, **83**, 5625-5632, 1978.

Fejer, B. G., The equatorial ionospheric electric fields : a review, *J. Atmos. Terr. Phys.*, **43**, 377-386, 1981.

Fejer, B. G., Equatorial ionospheric electric fields associated with magnetospheric disturbances, in *Solar-Wind-Magnetosphere Coupling*, Y. Kamide and J. A. Slavin (eds.), 519, Terra Scientific Publishing Co., Tokyo, 1986.

Fejer, B. G., and M. C. Kelley, Ionospheric irregularities, *Rev. Geophys. Space Phys.*, **18**, 401-454, 1980.

Fejer, B. G., D. T. Farley, P. Johnson, and J. Balsley, Type 1 radar echoes from the equatorial electrojet with double-peaked Doppler spectra, *J. Geophys. Res.*, **85**, 191-196, 1980.

Fessen, C. G., R. E. Dickinson, and R. G. Roble, Simulation of thermospheric tides at equinox with the National Center for Atmospheric Research general circulation model, *J. Geophys. Res.*, **91**, 4471-4489, 1986.

Fisk, L. A., R. L. Arnoldy, L. J. Lanzerotti, R. Linm, E. Oran, J. B. Reagan, M. Schulz, and B. T. Tsurutani, Chap. 9 in *Solar-Terrestrial Physics : Present and Future,* Butler D. M. and K. Papadopoulos (eds.), *NASA Ref. Publ. 1120,* Washington, D.C., 1984.

Foster, J. C., J. M. Holt, R. G. Klusgrove, and D. S. Evans, Ionospheric convection associated with discrete levels of particle precipitation, *Geophys. Res. Lett.*, **13,** 656-659, 1986.

Fremouw, E. J., C. L. Rino, R. C. Livingston, and M. C. Cousins, A persistent subauroral enhancement observed in Alaska, *Geophys. Res. Lett.*, **82,** 539-542, 1977.

Green, C. A., The semiannual variation in the magnetic activity indices A_a and A_p, *Planet. Space Sci.*, **32,** 297-305, 1984.

Harel, M., R. A. Wolf, P. M. Reiff, R. W. Spiro, W. J. Burke, F. J. Rich, and M. Smiddy, Quantitative simulation of a magnetospheric substorm. 1. Model logic and overview, *J. Geophys. Res.*, **86,** 2217-2241, 1981*a*.

Harel, M., R. A. Wolf, R. W. Spiro, P. M. Reiff, C.-K. Chen, W. J. Burke, F. J. Rich, and M. Smiddy, Quantitative simulation of a magnetospheric substorm. 2. Comparison with observations, *J. Geophys. Res.*, **86,** 2242-2260, 1981*b*.

Hedin, A. E., A revised thermospheric model based on mass spectrometer and incoherent scatter data : MSIS-83, *J. Geophys. Res.*, **88,** 10170-10188, 1983.

Huba, J. D., and S. I. Ossakow, On the generation of 3-m irregularities during equatorial spread-*F* by low-frequency drift waves, *J. Geophys. Res.*, **84,** 6697-6700, 1979.

Huba, J. D., and S. L. Ossakow, On 11-cm irregularities during equatorial spread *F*, *J. Geophys. Res.*, **86,** 829, 1981.

Kelley, M. C., and J. P. McClure, Equatorial spread-*F* : A review of recent experimental results, *J. Atmos. Terr. Phys.*, **43,** 427-435, 1981.

Kelley, M. C., R. C. Livingston, C. L. Rino, and R. T. Tsunoda, The vertical wave number spectrum of topside equatorial spread-*F* : estimates of backscatter levels and implications for a unified theory, *J. Geophys. Res.*, **87,** 5217-5221, 1982*a*.

Kelley, M. C., R. Pfaff, K. D. Baker, J. C. Ulwick, R. Livingston, C. Rino, and R. Tsunoda, Simultaneous rocket probe and radar measurements of equatorial spread-*F* transitional and short wavelength results, *J. Geophys. Res.*, **87,** 1575-1588, 1982*b*.

Kelley, M. C., J. F. Vickrey, C. W. Carlson, and R. Torbert, On the origin and spatial extent of high-latitute *F*-region irregularities, *J. Geophys. Res.*, **87,** 4469-4475, 1982*c*.

Keskinen, M. J., E. P. Szuszczewicz, S. L. Ossakow, and J. C. Holmes, Nonlinear theory and experimental observations of the local collisional Rayleigh-Taylor instability in a descending equatorial spread-*F* ionosphere, *J. Geophys. Res.*, **86,** 5785, 1981.

Krieger, A. S., A. F., Timothy, and E. C. Roelof, A coronal hole and its identification as the source of a high velocity solar wind stream, *Solar Phys.*, **29,** 505-525, 1973.

Leitinger, R., P. Wilkinson, and R. Hanbaba, The ionosphere in mid-latitudes during the SUNDIAL campaign, *Ann. Geophysicae*, **6,** 59-68, 1988.

Livingston, R. C., C. L. Rino, J. P. McClure, and W. B. Hanson, Spectral characteristics of medium-scale equatorial *F*-region irregularities, *J. Geophys. Res.*, **86,** 2421-2428, 1981.

Matsushita, S., and Y. Kamide, Penetration of high-latitude electric fields into low latitudes, *J. Atmos. Terr. Phys.*, **43,** 411-425, 1981*a*.

Matsushita, S., and Y. Kamide, Electromagnetic interactions between high and low latitudes shown by computer simulation movie, *J. Atmos. Terr. Phys.*, **43,** 403-410, 1981*b*.

Mayaud, P. N., Derivation, meaning and use of geometric indices, *Geophys. Monograph,* **22,** AGU, Washington, D.C., 1980.

McClure, J. P., W. B. Hanson, and J. H. Hoffman, Plasma bubbles and irregularities in the equatorial ionosphere, *J. Geophys. Res.*, **82,** 2650-2656, 1977.

Murayama, T., Coupling function between solar wind parameters and geomagnetic indices, *Rev. Geophys. Space Phys.*, **20,** 623-629, 1982.

Murayama, T., and N. Matuura, Longitudinal variability of annual changes in activity of equatorial spread-*F* and plasma bubbles, *J. Geophys. Res.*, **89,** 10903-10912, 1984.

Narcisi, R. S., Active Experiments, in *Space*, G. Haerendal (ed.), *ESA SP*-195, 1983.

Nichols, B. E., Tech. Note 1974-19, AF Contract F19628-73-C0002, Lincoln Laboratory, Bedford, Mass., 1974.

Nolte, J. T., A. S. Krieger, A. E. Timothy, R. E. Gold, E. C. Roelof, G. Vaiana, A. J. Lazarus, J. D. Sullivan, and P. S. McIntosh, Coronal holes as sources of solar wind, *Solar Phys.*, **46,** 303-307, 1976.

Ossakow, S. L., Spread-*F* theories — A review, *J. Atmos. Terr. Phys.*, **43,** 437, 1981.

Ossakow, S. L., W. Burke, P. Gary, R. Heelis, M. Keskinen, N. Mayguard, C. Meng, E. Szuszczewicz, and J. Vickrey, Chap. 12 in *Solar-Terrestrial-Physics,* Buttler D. M. and K. Papadopoulos (eds.), *NASA Ref. Publ. 1120,* Washington, D.C., 1984.

Perrault, P., and S. I. Akasofu, A study of geomagnetic storms, *Geophys. J. Roy. Astron. Soc.*, **54,** 547-554, 1978.

Pfaff, R. F., M. C. Kelley, B. G. Fejer, E. Kudeki, C. W. Carlson, A. Pedersen, and B. Hausler, Electric field and plasma density measurements in the auroral electrojet, *J. Geophys. Res.*, **89,** 236-244, 1984.

Rawer, K., International Reference Ionosphere-IRI 79, *NOAA Rep., UAG-82,* U.S. Dept. of Commerce, Washington, D.C., 1981.

Richmond, A. D., M. Blanc, B. A. Emery, R. H. Wand, B. G. Fejer, R. F. Woodman, S. Ganguly, P. Amayenc, R. A. Behnke, C. Calderon, and J. V. Evans, An empirical model of quiet-day ionospheric electric fields at middle and low latitudes, *J. Geophys. Res.*, **85,** 4658-4664, 1980.

Rino, C. L., R. T. Tsunoda, J. Petericks, and R. C. Livingston, Simultaneous rocket-borne beacon and *in situ* measurements of equatorial spread-*F* intermediate wavelength results, *J. Geophys. Res.*, **86,** 2411-2420, 1981.

Robinson, T. R., J. A. Waldock, M. D. Burrage, and T. B. Jones, High latitude ionospheric responses to changes in the interplanetary medium — SABRE observations during SUNDIAL, *Ann. Geophysicae,* **6,** 51-58, 1988.

Rodriguez, P., and E. P. Szuszczewicz, High-latitude irregularities in the lower *F*-region : intensity and scale size distributions, *J. Geophys. Res.*, **89,** 5575-5580, 1984.

Rodriguez, P., D. N. Walker, and E. P. Szuszczewicz, Auroral *F*-region irregularities correlated with geomagnetic activity, *NRL Memorandum* (in press), 1987.

Russel, C. T., The control of the magnetopause by the interplanetary magnetic field, in *Dynamics of the Magnetosphere,* S.-I. Akasofu (ed.), D. Reidel Publishing Co., Hingham, MA, 1980.

Schunk, R. W., and J. C. G. Walker, Theoretical ion densities in the lower ionosphere, *Planet. Space Sci.*, **21,** 1875-1896, 1973.

Schunk, R. W., and W. J., Raitt, Atomic nitrogen and oxygen ions in the daytime high-latitude *F*-region, *J. Geophys. Res.*, **85,** 1255-1272, 1980.

Schunk, R. W., and J. J. Sojka, Ion temperature variations in the daytime high-latitude *F*-region, *J. Geophys. Res.*, **87,** 5169-5183, 1982*a*

Schunk, R. W., and J. J. Sojka, Ionospheric hot spot at high latitudes, *Geophys. Res. Lett.*,, **9,** 1045-1048, 1982*b*.

Schunk, R. W., and E. P. Szuszczewicz, First principle and empirical modelling of the global-scale ionosphere, *Ann. Geophysicae,* **6,** 19-30, 1988.

Schunk, R. W., W. J. Raitt, and P. M. Banks, Effect of electric fields on the daytime high-latitude *E*- and *F*-regions, *J. Geophys. Res.*, **80,** 3121-3130, 1975.

Schunk, R. W., P. M. Banks, and W. J. Raitt, Effects of electric fields and other purposes upon the nighttime high-latitude *F*-layer, *J. Geophys. Res.*, **81,** 3271-3282, 1976.

Schunk, R. W., J. J. Sojka, and M. D. Bowline, Theoretical study of the electron temperature in the high-latitude ionosphere for solar maximum and winter conditions, *J. Geophys. Res.*, **91,** 12041-12054, 1986.

Schunk, R. W., A. R. Barakat, H. Carlson, J. B. Evans, J. Foster, R. Greenwald, M. C. Kelley, T. Potemra, M. H. Rees, A. D. Richmond, and R. G. Roble, Chap. 11 in *Solar-Terrestrial Physics : Present and Future,* Butler. D. M. and K. Papadopoulos (eds.) *NASA Ref. Publ. 1120,* Washington, D.C., 1984.

Singh, M., and E. P. Szuszczewicz, Composite equatorial spread-*F* wave number spectra from medium to short wavelengths, *J. Geophys. Res.*, **89,** 2313-2323, 1984.

Singh, M., P. Rodriguez, and E. P. Szuszczewicz, Spectral classification of medium-scale high-latitude *F*-region plasma density irregularities, *J. Geophys. Res.*, **90,** 6525-6532, 1985.

Sojka, J. J., and R. W. Schunk, A theoretical study of variations in response to magnetospheric storm inputs, *J. Geophys. Res.*, **89,** 2348-2358, 1984.

Sojka, J. J., and R. W. Schunk, A theoretical study of the global *F*-region for June solstice, solar maximum and low magnetic activity, *J. Geophys. Res.*, **90,** 5285-5298, 1985*a*.

Sojka, J. J., and R. W. Schunk, Theoretical study of anomalously high *F*-region peak altitudes in the polar ionosphere, *J. Geophys. Res.*, **90,** 7525-7532, 1985*b*.

Sojka, J. J., W. J. Raitt, and R. W. Schunk, A theoretical study of the high-latitude winter *F*-region at solar minimum for low magnetic activity, *J. Geophys. Res.*, **86,** 609-621, 1981*a*

Sojka, J. J., W. J. Raitt, and R. W. Schunk, Theoretical predictions for ion composition in the high-latitude winter *F*-region for solar minimum and low magnetic activity, *J. Geophys. Res.*, **86,** 2206-2216, 1981*b*.

Sojka, J. J., W. J. Raitt, and R. W. Schunk, Plasma density features associated with strong convection in the winter high-latitude *F*-region, *J. Geophys. Res.*, **86,** 6968-6976, 1981*c*.

Sojka, J. J., R. W. Schunk, and W. J. Raitt, Seasonal variations of the high-latitude *F*-region for strong convection, *J. Geophys. Res.*, **87,** 187-198, 1982.

Sojka, J. J., R. W. Schunk, and W. J. Raitt, A theoretical study of the high latitude *F*-region's response to magnetospheric storm inputs, *J. Geophys. Res.*, **88,** 2112-2122, 1983.

Spiro, R. W., M. Harel, R. A. Wolf, and P. H. Reiff, Quantitative simulation of a magnetic substorm. 3. Plasmaspheric electric fields and evolution of the plasmapause, *J. Geophys. Res.*, **86,** 2261-2272, 1981.

Spiro, R. W., R. A. Wolf, and B. G. Fejer, Penetration of high latitude electric field effects to low latitudes during SUNDIAL 1984, *Ann. Geophysicae,* **6,** 39-50, 1988.

Szuszczewicz, E. P., Ionospheric holes and equatorial spread-*F*: chemistry and transport, *J. Geophys. Res.*, **83,** 2665-2669, 1978.

Szuszczewicz, E. P., High latitude plasma dynamics : phenomenology, irregularity distributions, transport and magnetospheric coupling, App. C, 1-10, in *Solar-Terrestrial Physics-Workshop : Present and Future,* D. M. Butler and K. Papadopoulos (eds.) *NASA Ref. Publ. 1120,* Washington, D.C., 1984.

Szuszczewicz, E. P., J. C. Holmes, and M. Singh, The S3-4 ionospheric irregularities satellite experiment : probe detection of multi-ion component plasma and associated effects on instability processes, *Astrophys. Space Sci.*, **86,** 235-243, 1982.

Szuszczewicz, E. P., J. C. Holmes, and D. N. Walker, *Effect of the ionosphere on space and terrestrial system.* J. M. Goodman (ed.), U.S. Government Printing Office, 0-277-182, p. 220, 1978.

Szuszczewicz, E. P., R. T. Tsunoda, R. Narcisi, and J. C. Holmes, Coincident radar and rocket observations of equatorial spread-*F*, *Geophys. Res. Lett.*, **7,** 537-540, 1980.

Szuszczewicz, E. P., D. N. Walker, R. S. Narcisi, J. Buchau, B. Rhenisch, L. Kegley, and M. Swinney, Real-time *in situ* targeting of geoplasma domains for purposes of chemical injection and artificial triggering of equatorial spread-*F*, in *Active Experiments in Space,* G. Haerendel (ed.), *ESA SP-195,* ESA Technical Publications Branch, ESTEC, Noordwijk, Netherlands, 189-192, 1983.

Tsunoda, R. T., Backscatter measurements of 11-cm equatorial spread-*F* irregularities, *Geophys. Res. Lett.*, **1,** 848-850, 1980.

Tsunoda, R. T., Control of the seasonal and longitudinal occurrences of equatorial scintillations by the longitudinal gradient in integrated *E*-region Pedersen conductivity, *J. Geophys. Res.*, **90,** 447-456, 1985.

Tsunoda, R. T., M. J. Baron, J. Owen, and D. M. Towle, Altair — an incoherent scatter radar for equatorial spread *F* studies, *Radio Sci.*, **14,** 1111-1119, 1979.

Tsunoda, R. T., R. C. Livingston, J. P. McClure, and W. B. Hanson, Equatorial plasma bubbles : vertically elongated wedges from the bottomside *F*-layer, *J. Geophys. Res.*, 87, 9171-9180, 1982.

Viking Science Team, The Viking program, *EOS*, **67,** 793-795, 1986.

Wilkinson, P. J., R. W. Schunk, R. Hanbaba, and H. Mori, Interhemispheric comparison of SUNDIAL *F*-region data with global-scale ionospheric models, *Ann. Geophysicae,* **6,** 31-38, 1988.

Wolf, R. A., Ionosphere-magnetosphere coupling (review), *Space Sci. Rev.*, **17,** 537-562, 1975.

Wolf, R. A., M. Harel, R. W. Spiro, G. H. Voigt, P. H. Reiff, and C.-K. Chen, Computer simulation of inner magnetospheric dynamics for the magnetic storm of July 29, 1977, *J. Geophys. Res.*, **87,** 5949-5962, 1982.